ORIGINAL RESEARCH

Alkali induced changes in spatial distribution of functional groups in carboxymethylated cellulose

Paul Bogner · Thomas Bechtold · Tung Pham · Avinash P. Manian

Abstract The aim of the work was to investigate treatment parameters that exert most influence on performance of cellulose fibers carboxymethylated from aqueous solutions. Viscose fibers were carboxymethylated in alkaline solutions of sodium monochloroacetate at two temperatures (30 °C, 50 °C) and with different levels of alkali (0.5 mol/L and 4 mol/L NaOH). The degree of carboxymethylation was assessed with both back titration and conductometric titration methods, and the performance of carboxymethylated fibers was assessed from their propensity for sorption of the cationic dye methylene blue, a putative wastewater contaminant. Higher degrees of carboxymethylation were generally observed for fibers carboxymethylated in 4 mol/L NaOH, but in dye sorption propensities, the fibers carboxymethylated in 0.5 mol/L NaOH performed better. A combination of observations from dye sorption, color measurement and conductometric titration suggested that dye permeation was greater through fibers carboxymethylated in 0.5 mol/L NaOH as compared to 4 mol/L NaOH. As permeability differences were evinced in cases also where the degrees of carboxymethylation were very similar, it appears that the reaction conditions (i.e., alkali content during carboxymethylation), in addition to degree of carboxymethylation, affected fiber performance. The effect of alkali may stem from their influence on the topographical distribution of the substituted carboxymethyl functional groups.

Keywords Cellulose · Carboxymethylation · Alkali · Methylene blue sorption

P. Bogner · T. Bechtold · T. Pham · A. P. Manian (✉)
Research Institute of Textile Chemistry/Physics, Universität Innsbruck, Hoechsterstrasse 73, 6850 Dornbirn, Austria
e-mail: avinash.manian@uibk.ac.at

Introduction

As a renewable, biodegradable polymer that occurs abundantly in the biomass, there is significant interest in the use of cellulose to satisfy material needs. Apart from being used in its neat form, e.g. as cotton fibers, the chemical structure of the polymer is modified (i.e. cellulose is derivatized) to improve its suitability as required for different applications. The primary centers for chemical reactions are the three hydroxyl groups per D-glucose residue (or anhydroglucose unit) that are amenable to reactions such as etherification and esterification. Typical examples of commercially important cellulose derivatives are carboxymethyl cellulose and cellulose acetate, with production volumes per annum of about 600 000 tonnes and 2 000 000 tonnes respectively (Global Market Insights 2021; IMARC 2022).

🖄 Springer

Carboxymethyl cellulose (CMC), in the form of its sodium salt, has excellent water and moisture sorption properties and complexation ability (Heinze et al. 2018b). With sufficiently high degree of substitution, the sodium salt of CMC becomes water-soluble, and is used as thickening agent for viscosity modification, as dispersion agent, emulsion stabilizer, suspension agent in products such as paints, detergent formulations, and pharmaceutical formulations. In recent times, with growing emphasis on reducing the use of petroleum-based polymers and improving the eco-profile of processes, there is interest in expanding the use of CMC in more applications. Examples include as the absorbent in place of acrylate-based polymers in hygiene products (e.g. incontinence products) and as a binding agent for contaminants in wastewater remediation (Wang et al. 2019, 2023; Chen et al. 2022).

An issue to be addressed in such applications (absorbent, binding agent) is mechanical stability, to prevent displacement of the polymer from its intended location and for ensuring robust performance. The available options are to deposit and fix the polymer on a carrier (Ibrahim et al. 2020), to spin fibers from a dope of carboxymethylated cellulose that can then be assembled into fibrous networks (Wang et al. 2023), or first to assemble cellulose fibers into networks and then carboxymethylate them under heterogeneous conditions (Rácz et al. 1995). The third option is relevant for the textiles and nonwovens industries,

with their technological capabilities for large-scale chemical processing of two-dimensional assemblies of fibers.

A simplified illustration of cellulose carboxymethylation reaction is shown in Fig. 1. It is a Williamson-type etherification in presence of alkali (e.g. NaOH) involving the nucleophilic substitution at a cellulosic hydroxyl group of an alkyl halide, monochloroacetic acid. The addition of an alcohol (methanol, ethanol or isopropanol) to the reaction medium of aqueous alkali solution increases the degree of substitution as well as uniformity of functional group distribution through the cellulosic mass (Gu et al. 2012; Heinze et al. 2018b; Li et al. 2022; Liao et al. 2022; Liu et al. 2023; Thakur et al. 2023). The processing of two-dimensional substrates on a large scale, especially in open-width operations, frequently involves their transport through reaction media contained in open-to-air vessels. The use of alcohols is difficult under such circumstances, and thus aqueous reaction media of only alkali in water are preferred.

In aqueous media, the treatment parameters that can be adjusted for improving reaction yield are the reaction temperature, reagent amount, alkali amount and sequence of process steps. The yield increases with increase in reagent amount, and the temperature is adjusted to favor reagent reaction with cellulose over reagent hydrolysis in the reaction medium to sodium glycolate or disodium diglycolate, as illustrated in Fig. 1. Excellent reviews on the process
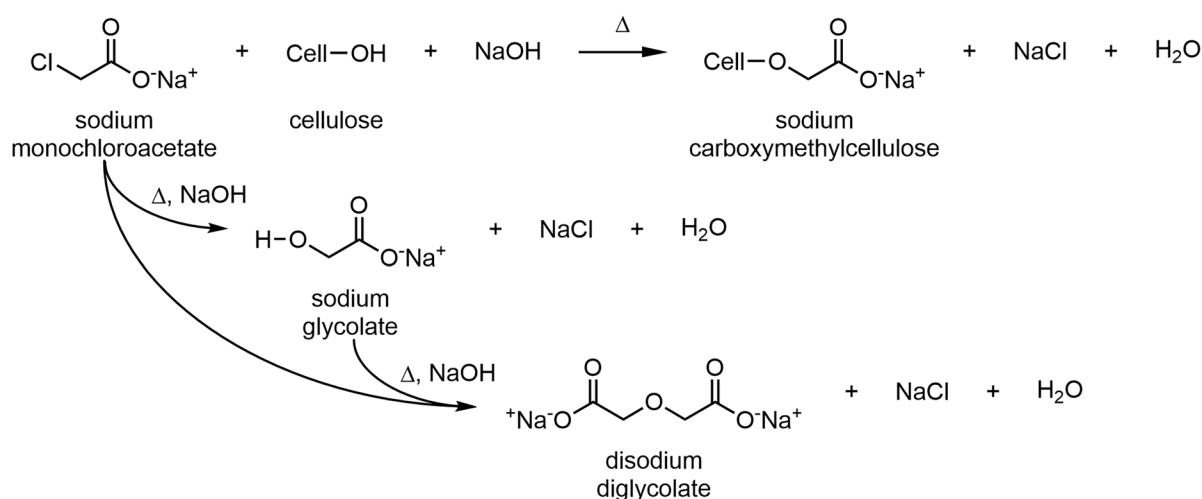

Fig. 1 Simplified illustration of cellulose carboxymethylation reaction

parameters and their influence are available in literature (Thielking and Schmidt 2006; Mischnick and Momcilovic 2010). The alkali, which is required to facilitate the reaction, may also act as an "activation" agent (Heinze et al. 2018a). Cellulose swells in alkali solutions, and the extents can range from inter-crystalline to intracrystalline swelling, depending on the type and concentration of alkali and the temperature. The former may lead to increase of porosity and the latter to both decrystallization and increase of porosity, all of which are conducive to increased reaction yields (Heinze et al. 2018a). The treatments may progress via first an activation step of the cellulose with alkali before introduction of the alkyl halide, first impregnation of the cellulose with the alkyl halide before introduction of the alkali, or introducing the cellulose into a bath containing both the alkali and alkyl halide.

The aim of this work was to determine influence of the variables listed above: reagent and alkali amounts, temperature, and treatment sequences on reaction yield, i.e., degree of carboxymethylation, and more importantly, on performance of the carboxymethylated cellulose fibers. The work was designed to identify underlying principles and mechanisms in carboxymethylation from entirely aqueous media, and it is to be noted that the reaction conditions employed are unsuited to be considered as a basis for commercialization.

The degree of carboxymethylation was determined from fiber carboxyl group contents measured with back titration, conductometric titration, and FTIR spectroscopy. Methylene blue dye sorption was used as a measure of performance, as the cationic dye is a widely used test substance in laboratory investigations on wastewater remediation (Rafatullah et al. 2010; Wang et al. 2023). The work was performed on viscose fibers, as it is widely used in the manufacture of products for use in technical, and hygiene and personal care applications (Krässig et al. 2004).

Materials

The viscose fibers of staple length 40 mm and fineness 1.7 dtex ("Danufil®") were kindly donated by Kelheim Fibres GmbH (Germany). The methylene blue was of pharmaceutical grade, spectroscopy grade KBr was used in FTIR transmission measurements,

while all other reagents were of analytical grade. Ultrapure water (LiChrosolv® grade) purchased from Merck KGaA (Germany) was used in conductometric titration, whereas deionized water of conductivity less than 10 μS/cm was employed in all other experiments.

Methods

Fiber cleaning

The viscose fibers were demineralized by immersion in 0.5 wt% HCl, with material-to-liquor ratio of 1:35, at 40 °C for 1 h. The fibers were drained, rinsed twice with deionized water, and immersed in 1 g/L sodium acetate for 30 min at 40 °C, with material-to-liquor ratio of 1:35. Then the fibers were drained, rinsed twice with deionized water and allowed to dry in ambient atmosphere for over four days.

Carboxymethylation

In all carboxymethylation reactions, 2 g demineralized fibers were treated in 120 mL aqueous reaction media containing 9 g sodium monochloroacetate (MCA), NaOH at concentration of either 0.5 mol/L or 4.0 mol/L, at temperature of either 30 °C or 50 °C. The treatment duration was 24 h, except in media containing 4 mol/L NaOH at 50 °C, where the duration was 4 h. A shortened duration was employed because it was determined previously that about 95% of the MCA was hydrolyzed within 4 h in media containing 4 mol/L NaOH at 50 °C.

Prior to the reaction step, the fibers underwent a pretreatment for 1 h, of:

- immersion in alkali alone (at the same temperature and NaOH concentration as in the reaction), or
- immersion in MCA alone (at the same temperature as in the reaction), or
- no pretreatment, i.e., the fibers were immersed directly into the reaction medium.

A summary of the treatment sequences is available in Table 1 and represented schematically in Fig. 2. In addition, two reference treatments were carried out for each combination of treatment variables, one with everything except the fiber (no-fiber

Table 1 Description of treatment sequences. In each, the same temperature was used in pretreatment and reaction steps, 30 °C or 50 °C

Label	Treatment sequence	
bp	Pretreatment	2 g fiber was immersed in 60 mL of NaOH solution (0.5 mol/L or 4 mol/L)
	Reaction	A liquor volume of 60 mL containing 9 g MCA and NaOH (0.5 mol/L or 4 mol/L) added to pretreatment mix
rp	Pretreatment	2 g fiber immersed in 60 mL deionized water containing 9 g MCA
	Reaction	A liquor volume of 60 mL containing NaOH (1 mol/L or 8 mol/L) added to pretreatment mix
np	Pretreatment	None
	Reaction	2 g fiber immersed in liquor volume of 120 mL containing 9 g MCA and NaOH (0.5 mol/L or 4 mol/L)

Duration of the pretreatment step was always 1 h. The reaction step duration was 24 h in all instances except with 4 mol/L NaOH at 50 °C, where the duration was 4 h
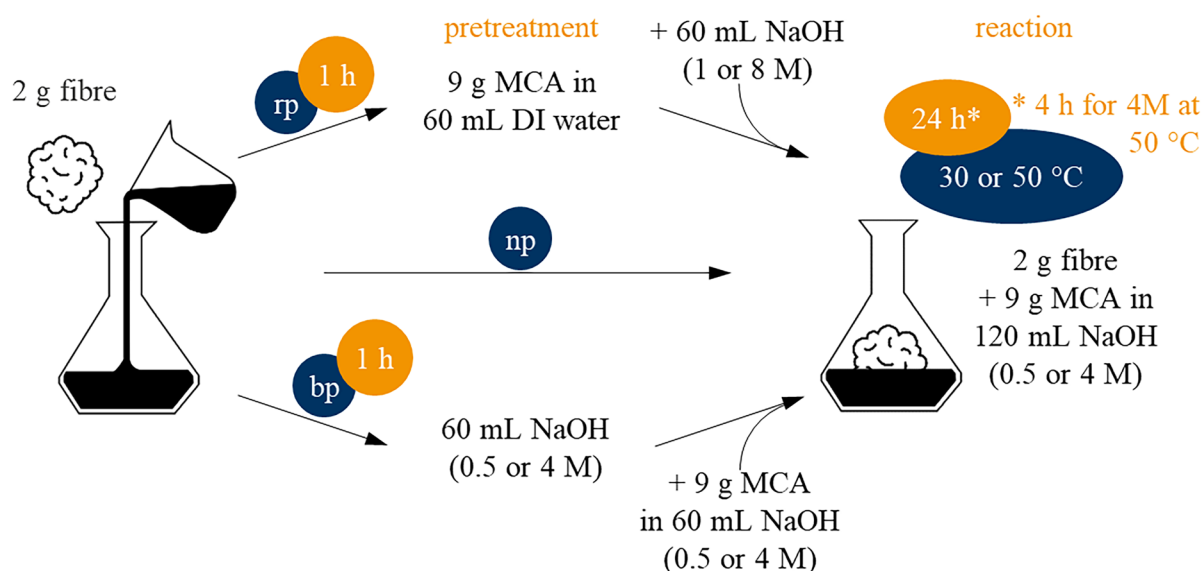
Fig. 2 Schematic representation of treatment sequences. Explanations of the terms *rp*, *np* and *bp* are available in Table 1. Illustrations of the fiber bundle and reaction vessels are reproduced under CC BY license from the work of Tyler Gobberdiel and Michael Zick Doherty respectively, available at the Noun Project (https://thenounproject.com/)

blank, "*nf*-blank") and the other with everything except the MCA (no-MCA blank).

All pretreatments and reactions were performed under constant agitation. After, the fibers were separated from the media, immersed in 1 mol/L of acetic acid for 1 h to neutralize the alkali, drained, and rinsed with deionized water for washing off residual salts. The fibers were then put in filtration tubes of porosity 10 μm, centrifuged at 4000×*g* for 10 min to drain excess water, and dried in ambient atmosphere.

Analysis of reaction media

The residual alkali in reaction media was determined by acid–base titration with a standardized solution of 1 mol/L HCl. The chloride content was determined as per DIN 38405–1 (DIN 1985) by potentiometric titration with a standardized solution of 0.1 mol/L AgNO$_3$.

The contents of glycolic acid, diglycolic acid and residual MCA were determined with high-performance liquid chromatography (HPLC) on a Aminex

HPX-87H column (Bio-Rad Laboratories Inc., USA) with UV detection at 210 nm in a Nexera XR device equipped with a SPD-M20A photodiode array detector (Shimadzu Europa GmbH, Germany). The samples were acidified to pH 3 with 0.3 mol/L H_2SO_4 prior to analysis, and 3 mmol/L H_2SO_4 was used as eluent at 0.6 mL/min flow rate with oven temperature of 35 °C.

Fiber analysis

The method of methylene blue sorption followed that described in literature (Klemm et al. 1998). About 0.1–0.2 g specimens were agitated for 24 h at room temperature in 50 mL liquor composed of 25 mL methylene blue solution (of 300 mg/L) and 25 mL borate buffer at pH 8.5 (of 1 mol/L boric acid and 0.25 mol/L NaOH). The residual content of methylene blue content in liquor at the end was quantified photometrically (at 665 nm) and used in calculation of the carboxyl group content with Eq. 1.

$$COOH = \left[\frac{(7.5 - A) \times 0.00313}{E} \right] \times 10^3 \quad (1)$$

where $COOH$ = carboxyl group content of specimen (mmol/kg), A = residual content of methylene blue (mg), E = specimen mass (g).

The dyed fibers were rinsed with deionized water and dried in ambient atmosphere, before their reflectance spectra were measured with specular component excluded on a d/8 spectrophotometer (Model CM-3610d, Konica Minolta Sensing Europe B.V., The Netherlands) in 10 nm intervals over the range 400–740 nm. The measured reflectance was converted to K/S values with the Kubelka–Munk function (Eq. 2), and their average (K/S_{av}) was calculated with Eq. 3. A shift in the wavelength of maximum absorbance was observed with increasing degree of carboxymethylation, and that was quantified by means of the spectral centroid (λ_{sc}) as shown in Eq. 4 (Stone 1967).

$$K/S_\lambda = \frac{(1 - R_\lambda)^2}{2R_\lambda} \quad (2)$$

$$K/S_{av} = \frac{\sum K/S_\lambda}{n_\lambda} \quad (3)$$

$$\lambda_{sc} = \frac{\sum (K/S_\lambda \cdot \lambda)}{\sum K/S_\lambda} \quad (4)$$

where $K/S_\lambda = K/S$ at wavelength λ, R_λ = fractional reflectance at wavelength λ, K/S_{av} = average K/S, n_λ = number of measurements in the 400–740 nm range (=35), λ_{sc} = spectral centroid, measure of shift in absorbance peak.

The procedure for conductometric titration was based on descriptions in literature (Sjostrom and Enstrom 1966; Katz and Beatson 1984; Fras et al. 2004). About 0.5 g specimens were placed in a cage of polypropylene mesh, immersed in 500 mL solution containing 1 mmol/L NaCl with 1 mL of 0.1 mol/L HCl. They were titrated with NaOH of concentration 10–50 mmol/L in increments of 0.15–0.3 mL per 30–900 s under continuous stirring and monitoring of conductance until a pH of 10.5. Ultrapure water was used in these measurements. To minimize the effects of Na_2CO_3 contamination on the results, NaOH pellets were first rinsed with ultrapure water to wash out approximately 50–75% of the solids, before dissolving the rest to formulate the titrant solutions. The resulting concentration of NaOH was determined by titration with oxalic acid dihydrate.

The back titration method was derived from the TAPPI standard T237 om-08 (TAPPI 2008). The specimens were first protonated by immersion and agitation in 0.1 mol/L HCl for 2 h (about 0.5 g in 50 mL). They were then filtered under vacuum, rinsed thrice with carbonated deionized water prepared in a home soda-maker from SodaStream International Ltd (Israel), and vacuum filtered again. This step was undertaken to ensure complete protonation of carboxyl groups in fibers. The specimens were then transferred to another vessel containing 50 mL of 0.01 mol/L $NaHCO_3$ with 0.1 mol/L NaCl, agitated for 60 min, and filtered. The filtrates (25 mL volume) were titrated with a standardized solution of 0.01 mol/L HCl, a separate titration of the original $NaHCO_3 + NaCl$ solution was performed as blank, and the specimen carboxyl contents were calculated with Eq. 5.

$$COOH = \left[(0.05 \times C_B) - (2 \times 0.025 \times C_F) \right] \times \frac{1}{m} \times 10^6 \quad (5)$$

where $COOH$ = carboxyl group content of specimen (mmol/kg), C_B = Concentration of $NaHCO_3$ in

the blank (mol/L), C_F = Concentration of $NaHCO_3$ in the filtrate (mol/L), m = specimen mass (g), *0.05* = volume of $NaHCO_3$ + NaCl solution in which specimens were agitated (L), *0.025* = volume of $NaHCO_3$ + NaCl filtrate used in titration (L).

FTIR spectra, in both Attenuated Total Reflectance (ATR) and transmission modes, were recorded on an Invenio S spectrometer (Bruker Optik GmbH, Germany) from an aggregate of 128 scans between 4000 and 600 cm^{-1} at a resolution of 2 cm^{-1}. Prior to measurements, specimens were deprotonated by immersion and agitation in 0.1 mol/L NaOH, at material-to-liquor ratio 1:100, in ambient temperature for 1 h, taken out, rinsed with deionized water, filtered under centrifugation at $4000 \times g$ for 10 min, and dried in ambient atmosphere.

The ATR measurements were performed directly on a small bundle of fibers with aid of a MIRacle™ Horizontal ATR accessory fitted with a diamond crystal double reflection universal plate from PIKE Technologies (USA). For transmission measurements, the specimens were integrated into KBr pellets. About 50 mg of specimens were ground for 10 min in liquid nitrogen on a vibratory cryomill with a zirconium oxide grinding set (Pulverisette 0, Fritsch GmbH, Germany), and dried for 3 h at 110 °C. The KBr was ground by hand in an agate mortar and pestle and dried for 3 h at 110 °C. About 3 mg of the ground specimen was mixed with about 300 mg of the ground KBr, ground together for 3 min in an agate set on a ball mill (Specamill, Graseby-Specac, England), and dried again for 60 min at 110 °C. The mixtures were then transferred into a pellet die of 13 mm diameter and subjected to 10-ton load for 10 min, under evacuation (< 100 mbar), in a hydraulic press (both die and press from Specac, England). The pellets so formed were immediately utilized for spectroscopy.

Results and discussion

Reaction media analyses

The results from analyses of residual NaOH, unreacted MCA, chloride content, glycolic acid and diglycolic acid in reaction media after fiber treatments, are available in Table 2. There were no significant differences in the measured contents within a NaOH/temperature combination, and hence the values presented are averages across the treatment sequences. Similarly, the values presented for no-fiber blanks are also averages across treatment sequences as no significant differences were observed between them.

Table 2 Results of reaction media analyses. Mean values from three replicates are shown along with their standard deviation (in parentheses)

Treatment variables			Contents in residual reaction media				
NaOH (mol/L)	Temp. (°C)	Sequence	NaOH (mol/L)	MCA[a] (mol/L)	Cl^{-}[b] (mol/L)	GA[c] (mol/L)	dGA[d] (mol/L)
0.5	30	*bp, rp, np*	0.362 (0.003)	0.519 (0.011)	0.109 (0.008)	0.108 (0.008)	0.001 (0.001)
		nf-blank[e]	0.378 (0.008)	0.509 (0.018)	0.111 (0.008)	0.111 (0.007)	0.001 (0.001)
	50	*bp, rp, np*	0.128 (0.006)	0.281 (0.008)	0.341 (0.016)	0.318 (0.006)	0.009 (0.0004)
		nf-blank	0.136 (0.006)	0.272 (0.010)	0.356 (0.015)	0.328 (0.007)	0.010 (0.0004)
4	30	*bp, rp, np*	3.207 (0.117)	*nd*[f]	0.642 (0.026)	0.505 (0.007)	0.058 (0.001)
		nf-blank	3.246 (0.195)	*nd*	0.646 (0.022)	0.513 (0.0002)	0.059 (0.001)
	50	*bp, rp, np*	3.092 (0.160)	*nd*	0.630 (0.032)	0.522 (0.017)	0.047 (0.001)
		nf-blank	3.156 (0.213)	*nd*	0.659 (0.049)	0.554 (0.030)	0.052 (0.008)

[a]Unreacted MCA; [b]chloride; [c]glycolic acid; [d]diglycolic acid; [e]no-fiber blank; [f]not detectable

The aim of these analyses was to estimate the degree of fiber carboxymethylation for comparison with carboxyl group content analyses on the treated fibers. However, that was found not possible because there were generally no significant differences between the results from fiber treatments and no-fiber blank experiments.

The proportions of unreacted MCA decreased with rise in temperature of media in the 0.5 mol/L NaOH treatments, from *ca*. 80% at 30 °C to *ca.* 43% at 50 °C, whereas in all treatments with 4 mol/L NaOH, no unreacted MCA was detectable in the residual media. The residual NaOH contents in reaction media with fibers were lower than in the corresponding no-fiber blanks and that is attributed to sorption by the cellulose.

The chloride content represents the total degree of MCA hydrolysis, and together with amounts of unreacted MCA, the values accounted for on average *ca.* 98–99% of the initial MCA content (of 0.644 mol/L) in all results. The contents of glycolic and diglycolic acid together, represent the MCA hydrolyzed in reaction media but without reacting with the cellulose. These values accounted for on average *ca.* 99% of the chloride content. Thus, although the reaction media analyses yielded information on the degree of MCA hydrolysis as function of the treatment variables, not much information could be discerned on its extent of reaction with cellulose.

Fiber analysis

Results from carboxyl content determinations, methylene blue dye sorption and FTIR spectroscopy derived normalized absorbance intensities are shown in Table 3. The average carboxyl contents, as measured through back titration, ranged from 64 to 623 mmol/kg. The highest values were observed through reactions in 4 mol/L NaOH, with lower temperatures resulting in higher carboxyl contents. The *rp* sequence produced greater values than the *np* and *bp* sequences. Samples from treatments in 0.5 mol/L NaOH exhibited lower carboxyl contents, higher temperatures resulted in higher carboxyl contents, and no significant differences were observed between the different reaction sequences. The no-MCA blank and demineralized samples showed the lowest carboxyl contents.

The results of the performance analysis, in terms of methylene blue dye sorption levels, are shown in Fig. 3a. In principle, the sorption is governed by electrostatic interactions with a 1:1 stoichiometry between the cationic dye and anionic carboxylate group (Stone and Bradley 1967), as illustrated schematically in Fig. 4. However, the results showed that dye sorption levels increasingly diverged from a 1:1 relationship with rise in the degree of carboxymethylation. A "*saturation*" became apparent at carboxyl content of *ca.* 373 mmol/kg, corresponding to fibers carboxymethylated in 0.5 mol/L NaOH at 50 °C, with further rise in the degree of carboxymethylation producing no improvements in dye sorption levels. To confirm if the carboxyl contents as determined with back titration were indeed accurate, the samples were analyzed for carboxyl content also with conductometric titration, and the results are shown in Fig. 3b. Overall, there was close correlation between values from conductometric and back titration across the entire range of measurements, which acted to validate the carboxyl content determinations.

More data points were deemed desirable to better characterize the obtained dye sorption profile (Fig. 3a). To that end, additional carboxymethylation treatments were performed in 4 mol/L NaOH at 30 °C and 50 °C using the *np* sequence, with half and quarter of the MCA levels used in all other reactions, i.e. with MCA contents of 0.161 mol/L and 0.322 mol/L in reaction media. Increasing the MCA content beyond 0.644 mol/L was not found feasible under the conditions used in this work, due to solubility limitations of the reagent. The samples were analyzed as all others, and the results are shown in Table S1 (Online Resource 1). The carboxyl contents determined with conductometric titration showed the same close correspondence to carboxyl contents derived from back titration (see Fig. S1, Online Resource 1).

The dye sorption profile including results of samples from the additional treatments is shown in Fig. 5. The sorption of methylene blue dye on CMC is characterized by the Type I or Langmuir isotherm (Yan et al. 2011; Siswanta et al. 2020; Gago et al. 2020; Li et al. 2023), that implies site-specific sorption of adsorbate as a monolayer, that ultimately leads to saturation. The dye sorption profiles in Figs. 3 and 5, although not isotherm plots, are consistent with saturation levels being reached in the dye uptake. Whereas the results in Fig. 3 suggested a uniform

Table 3 Results of carboxyl group content, methylene blue sorption measurements and normalized FTIR absorbance intensities on fibers. Mean values from three replicates are shown along with their standard deviation (in parentheses)

Treatment variables			Carboxyl group content (mmol/kg)		MB Sorption (mmol/kg)[c]	Normalized FTIR absorbance[d]	
NaOH (mol/L)	Temp. (°C)	Sequence	A-B[a]	Cond.[b]		ATR	KBr
0.5	30	*bp*	169.6 (1.6)	135.9 (4.7)	52.8 (13.6)	0.358 (0.003)	0.327 (0.022)
		rp	181.4 (1.6)	132.1 (11.8)	45.8 (5.2)	0.358 (0.004)	0.285 (0.003)
		np	171.0 (0.8)	148.6 (4.7)	44.6 (8.4)	0.371 (0.006)	0.321 (0.036)
	50	*bp*	367.6 (1.9)	324.1 (6.2)	97.0 (1.5)	0.642 (0.014)	0.455 (0.027)
		rp	374.4 (3.8)	319.6 (12.1)	92.7 (3.2)	0.614 (0.011)	0.452 (0.007)
		np	377.3 (2.3)	328.1 (21.4)	98.3 (3.0)	0.639 (0.012)	0.467 (0.018)
4	30	*bp*	555.4 (20.6)	455.6 (13.9)	92.5 (1.6)	0.982 (0.017)	0.737 (0.005)
		rp	623.3 (2.4)	582.2 (11.8)	85.4 (0.4)	1.033 (0.048)	0.707 (0.026)
		np	545.4 (6.8)	522.6 (62.8)	87.6 (1.8)	0.978 (0.029)	0.696 (0.097)
	50	*bp*	462.9 (31.0)	301.0 (84.8)	88.8 (2.1)	0.888 (0.017)	0.730 (0.166)
		rp	494.5 (21.1)	319.9 (47.7)	77.5 (3.9)	0.881 (0.049)	0.683 (0.010)
		np	449.1 (45.3)	379.7 (42.2)	83.6 (4.3)	0.878 (0.004)	0.512 (0.0005)
No-MCA blank[e]			63.7 (10.0)	50.3 (7.5)	14.8 (8.5)	0.156 (0.057)	–[f]
Demineralized fibers			67.5 (0.4)	41.1 (1.5)	7.8 (0.5)	0.207 (0.026)	0.172 (0.057)

[a]back titration, [b]conductometric titration, [c]methylene blue sorption, [d]absorbance intensities at 1591 cm^{-1} (ATR) and 1600 cm^{-1} (KBr, i.e. transmittance) normalized with respect to the absorbance intensity at 1156 cm^{-1}, [e]the values shown are the means from no-MCA blank experiments across all combinations of treatment variables and sequences, [f]signifies not measured

relationship between dye sorption and degree of carboxymethylation, with the additional data points included in Fig. 5, differences appear between fibers carboxymethylated in 0.5 mol/L NaOH vs. 4 mol/L NaOH. Compared to fibers reacted in 4 mol/L NaOH, the fibers reacted in 0.5 mol/L NaOH exhibited higher dye sorption and a greater rate of change in dye sorption levels with degree of carboxymethylation, and although measurements are not available, it appears that the saturation levels in the fibers may also be higher. The carboxyl content was higher in fibers carboxymethylated in media with 4 mol/L NaOH, but it appears that a greater proportion of carboxyl groups were available for dye sorption in fibers carboxymethylated in 0.5 mol/L NaOH.

The differences of carboxymethyl group availability may relate to their distribution through fiber structures, and that may be assessed with FTIR spectroscopy, where absorbance peaks attributed to cellulose carboxylate groups are observed in the region of 1600 cm^{-1} (Mohkami and Talaeipour 2011; Li et al. 2020). If the carboxylate peak intensity is normalized with respect to the peak intensity at 1156 cm^{-1}, attributed to asymmetric stretching of the C—O—C glycosidic linkage (Marchessault and Liang 1960; Carrillo et al. 2004), the value serves as an index of the proportion (or density) of carboxylate groups in a cellulose sample. The normalized intensities from measurements in the ATR mode are representative of the "*surface*" density and transmission mode measurements are representative of "*bulk*" density (Wang 2017).

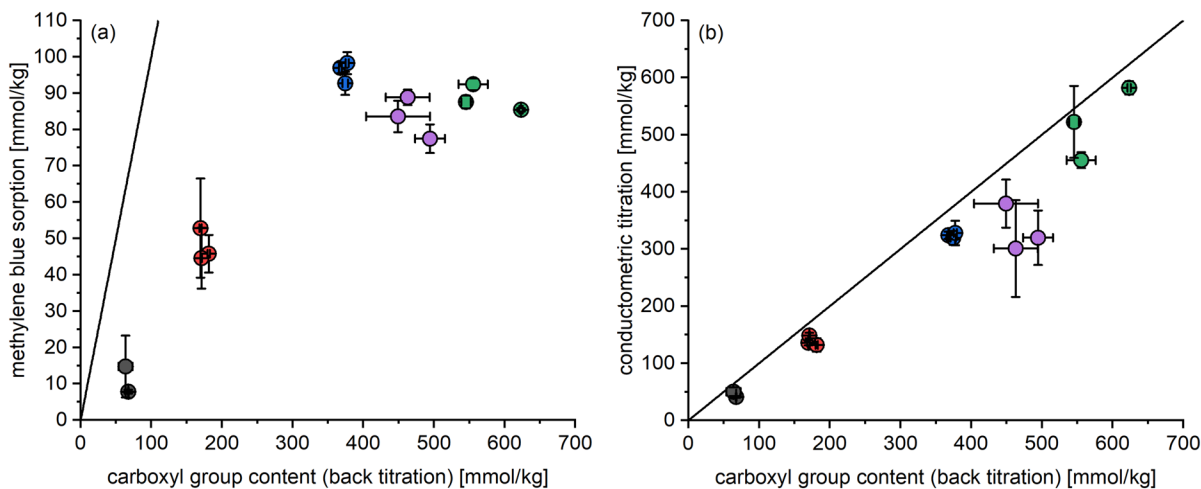The FTIR spectra in the region between 1500 and 1800 cm^{-1}, from measurements in ATR mode and

Fig. 3 a Levels of methylene blue dye sorption plotted against carboxyl contents as determined with back titration, **b** Comparison of carboxyl contents determined with conductometric titration vs. back titration. The diagonal line in each plot represents a 1:1 relationship between the abscissa and ordinate. The marker colors represent treatment sets: demineralized and no-MCA blank (grey circle), in 0.5 mol/L NaOH at 30 °C (orange circle), in 0.5 mol/L NaOH at 50 °C (blue circle), in 4 mol/L NaOH at 30 °C (green circle) and in 4 mol/L NaOH at 50 °C (violet circle)

Fig. 4 Schematic illustration of interaction between carboxylate group and methylene blue cation (MB +)
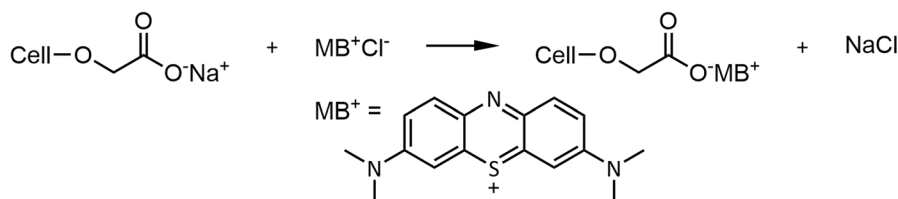
transmittance mode, of selected samples from this work, are shown in Fig. S2 (Online Resource 1). The carboxylate absorbance peak appeared at 1591 cm^{-1} in ATR mode measurements and at 1600 cm^{-1} in transmission mode measurements. Small peak shifts are commonly observed between ATR and transmission measurements in FTIR spectroscopy, and attributed to the effects of sample thickness and refractive index in ATR measurements (Harrick and du Pré 1966; Nunn and Nishikida 2008). The normalized peak intensities are plotted as function of carboxyl content in samples determined with back titration, in Fig. 6.

The normalized ATR intensities increased near-linearly with fiber carboxyl content. The normalized transmittance intensities were initially very close to the normalized ATR intensities, but diverged to lower values with rise in fiber carboxyl contents. It suggests a uniform distribution of carboxyl group density through fiber structures in control samples and in samples carboxymethylated up to *ca.* 200 mmol/kg, but with rise in degree of carboxymethylation, the surface density of carboxylate groups exceeded that of the bulk density. In other words, with increase in the extent of derivatization, the reactions appear to have proceeded to greater extents on fiber surfaces than in the fiber bulk. It may be noted that no clear influence was observed of the reaction conditions (e.g. alkali content in reaction media) on the differences between the normalized intensities. Comparisons of ATR and transmission spectra in FTIR spectroscopy, for assessing uniformity of functional group distribution in polymeric materials, are reported also elsewhere (Gogna and Goacher 2018; Liu and Kazarian 2022; Manian et al. 2022).

However, when the dye sorption levels in fibers were plotted against their normalized ATR intensities, i.e. surface density of carboxyl groups, the rate of
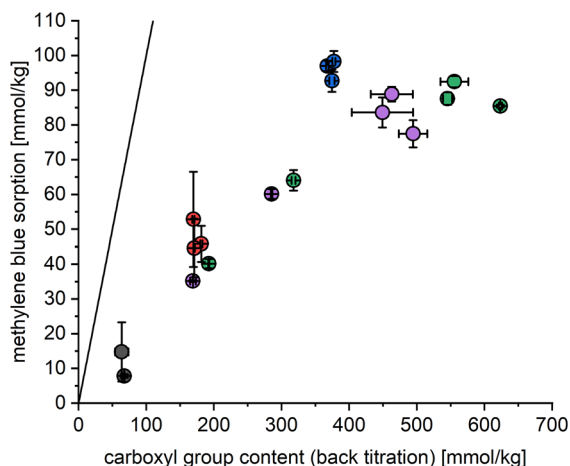
Fig. 5 Plot of methylene blue sorption vs carboxyl contents measured with back titration, including data from the additional treatments. The diagonal line represents a 1:1 relationship between the abscissa and ordinate. The marker colors represent treatment sets: demineralized and no-MCA blank (grey circle), in 0.5 mol/L NaOH at 30 °C (orange circle), in 0.5 mol/L NaOH at 50 °C (blue circle), in 4 mol/L NaOH at 30 °C (green circle) and in 4 mol/L NaOH at 50 °C (violet circle)
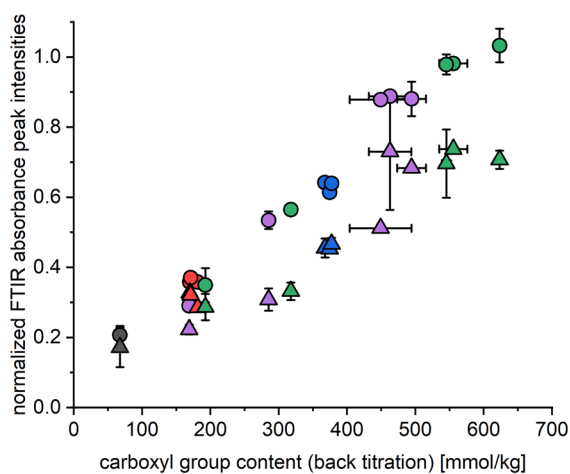
Fig. 6 Absorbance peak intensities at 1591 cm^{-1} and 1600 cm^{-1} from ATR and transmission spectra respectively, normalized with respect to the corresponding intensities at 1156 cm.$^{-1}$. The circles are data from ATR spectra, and the triangles from transmission spectra. The marker colors represent treatment sets: demineralized and no-MCA blank (grey circle, grey triangle), in 0.5 mol/L NaOH at 30 °C (orange circle, orange triangle), in 0.5 mol/L NaOH at 50 °C (blue circle, blue triangle), in 4 mol/L NaOH at 30 °C (green circle, green triangle) and in 4 mol/L NaOH at 50 °C (violet circle, violet triangle)

change in dye sorption with change in surface density of carboxyl groups appeared to be greater for fibers carboxymethylated in 0.5 mol/L NaOH (see Fig. 7). A possible explanation is that in FTIR-ATR measurements, the depth of incident beam penetration into substrates may range between 0.5 and 5 μm (Anon 2023). Thus, the signal intensity will be proportional to all available functional groups in that range of depth in samples, but perhaps the dye molecules did not have similar access to all functional groups in that space.

Additional information may be obtained from examination of the light reflectance data. The transformation of reflectance to K/S_λ with Eq. 2 yields a measure of the absorbance intensity at each measured wavelength, whereas K/S_{av} values calculated with Eq. 3 yield measures of the overall absorbance intensity, which may also be referred to as the color intensity. As seen in Fig. 8a, the color intensity increased with rising dye sorption in all samples, but the rate of change appeared greater for samples carboxymethylated in 4 mol/L NaOH as compared to 0.5 mol/L NaOH. Further, for the same level of methylene blue sorption, especially towards the upper range of vales, the K/S_{av} values were greater for fibers carboxymethylated in 4 mol/L NaOH. In opaque solids such as
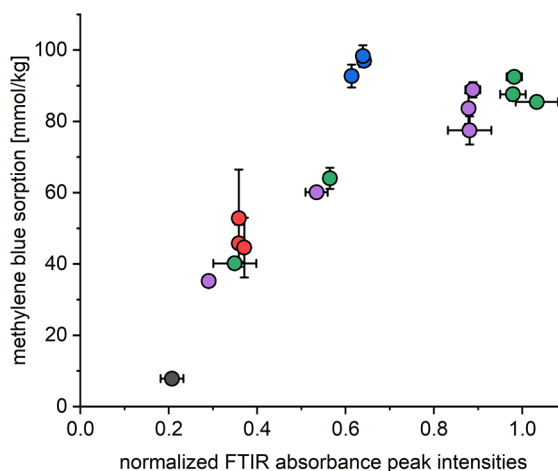

Fig. 7 The levels of methylene blue sorption in fibers plotted vs. their normalized ATR intensities. The marker colors represent treatment sets: demineralized and no-MCA blank (grey circle), in 0.5 mol/L NaOH at 30 °C (orange circle), in 0.5 mol/L NaOH at 50 °C (blue circle), in 4 mol/L NaOH at 30 °C (green circle) and in 4 mol/L NaOH at 50 °C (violet circle)
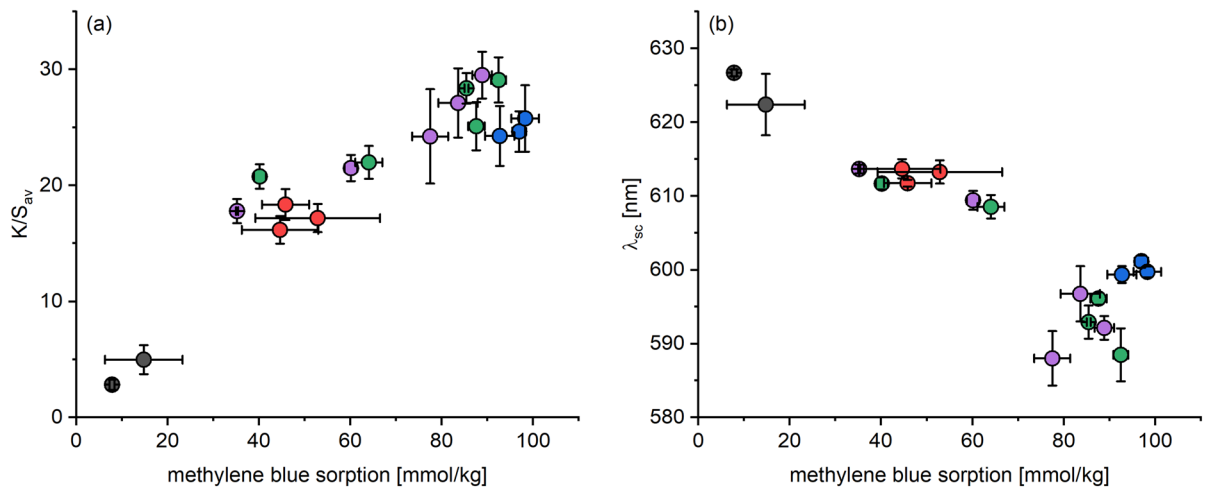
Fig. 8 Profiles of color intensity, i.e. K/S_{av} (**a**), and spectral centroid, λ_{sc} (**b**) vs. methylene dye sorption in fibers. The marker colors represent treatment sets: demineralized and no-MCA blank (grey circle), in 0.5 mol/L NaOH at 30 °C (orange circle), in 0.5 mol/L NaOH at 50 °C (blue circle), in 4 mol/L NaOH at 30 °C (green circle) and in 4 mol/L NaOH at 50 °C (violet circle)

fibers, the color intensity is proportional to colorant amounts at or near their surfaces. Thus, the results indicate a greater accumulation of the methylene blue dye at or near the surface in samples carboxymethylated in reaction media containing 4 mol/L NaOH.

Further, a hypsochromic shift, i.e. shift of absorbance peak to lower wavelengths, was observed in the spectrum of the methylene blue adsorbed samples, which resulted in a change of the color (see Fig. S3, Online Resource 1). The phenomenon, termed metachromasy, is known to occur with methylene blue dye adsorbed on cellulose polyanions including carboxymethyl cellulose (Pal 1958; Bergeron and Singer 1958; Lawton and Phillips 1982). There are differences between polyanions (e.g. sulfate, phosphate, carboxymethyl), but for any given polyanion, the level of metachromasy increases with the degree of close packing between the adsorbed cationic dye molecules. The metachromasy levels observed in the samples of this work, calculated with Eq. 4, is shown in Fig. 8b as function of dye sorption levels. It may be observed that the fibers carboxymethylated in 4 mol/L NaOH exhibit greater levels of metachromasy per unit change in dye sorption levels.

Thus, the dye sorption levels were lower in samples carboxymethylated in reaction media with 4 mol/L NaOH despite the carboxyl contents being higher, and the K/S_{av} values and metachromasy levels

suggest that the adsorbed dye molecules accumulated near the surface to greater extents than in fibers carboxymethylated in media containing 0.5 mol/L NaOH. That suggests lower levels of dye permeation through fiber structures carboxymethylated in media containing 4 mol/L NaOH.

Some insights are available from conductometric measurements, in the profiles of change in solution conductance vs. added titrant amount and the corresponding measurement durations (see Fig. 9). As shown in part (a), the carboxyl contents are derived from the intersection points of three linear segments in the profile of change in conductance with addition of titrant. The first segment, of decreasing conductance, results from progressive neutralization of excess acid in the titration bath. The second segment, where the conductance generally changes little, results from deprotonation of carboxyl groups on the cellulose. The third segment, of increasing conductance, results from an increasing presence of excess alkali in the titration bath. The carboxyl content is determined by the length of the second segment between its intersection points with the first and third segments, representing the titrant amount consumed in deprotonation.

To obtain clear and sharp transitions from one segment to the other, it is necessary at each step to ensure equilibration of the added titrant with reactants in the titration bath (excess acid, cellulosic carboxyl
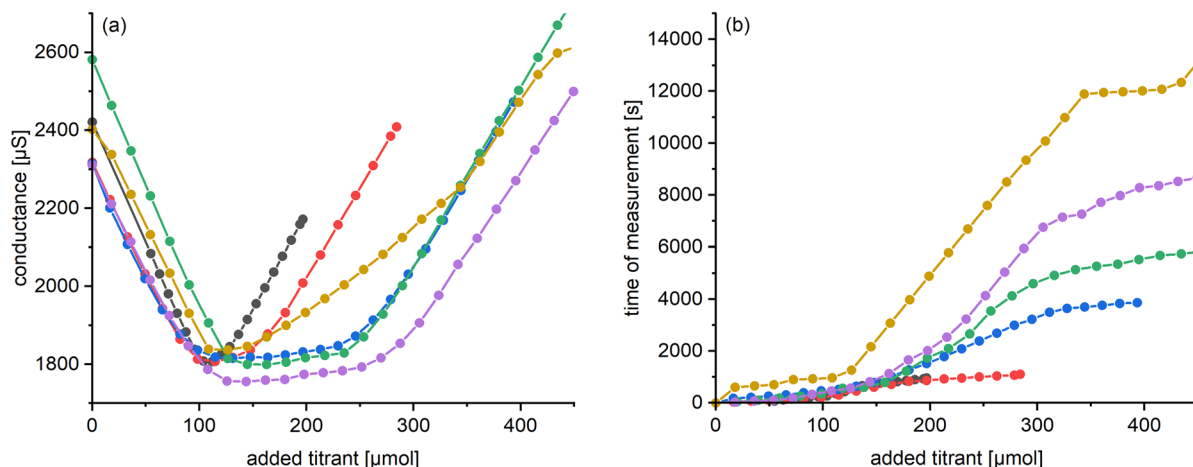
Fig. 9 Profiles of conductance in titration bath vs. amount of added titrant (**a**) and the corresponding time required per measurement point (**b**), from selected conductometric titration measurements. The colors signify different treatment sequences and their resulting carboxyl contents: no-MCA blank, 63.7 mmol/kg (grey circle); 0.5 mol/L NaOH at 30 °C, 169.6 mmol/kg (orange circle); 0.5 mol/L NaOH at 50 °C, 367.6 mmol/kg, (blue circle); 4 mol/L NaOH at 30 °C, 317.7 mmol/kg (green circle); 4 mol/L NaOH at 50 °C, 449.1 mmol/kg (violet circle); 4 mol/L NaOH at 50 °C, 462.9 mmol/kg (yellow circle)

groups), prior to any subsequent addition. That is rapidly achieved in the first segment during the phase of excess acid neutralization, but may be slower in the second segment during the phase of carboxyl group deprotonation as it involves alkali permeation through the fiber structure. Too rapid a rate of titrant addition is characterized by non-linear segments in the second phase as well as uncertainties in establishing the point of transition to the third phase.

In the conductometric titrations, settings defining equilibration as change in conductance of less than $0.1 \mu S/6$ s with durations of 30–300 s between additions, was sufficient to yield acceptable profiles of the change in conductance in measurements on demineralized fibers and those carboxymethylated in 0.5 mol/L NaOH. However, that proved not to be suitable for fibers carboxymethylated in 4 mol/L NaOH. Hence, the settings were modified to define equilibration as change in conductance of less than $0.1 \ \mu S/10$ s, with durations of 30–900 s between additions. The conductometric measurements were far slower on fibers carboxymethylated in reaction baths with higher alkali content, as can be seen in Fig. 9 showing comparisons between the measurement profiles of demineralized fibers and samples carboxymethylated in 0.5 mol/L NaOH and 4 mol/L NaOH. As illustration, of two samples showing similar carboxyl contents, of 367.6 mmol/kg and 317.7 mmol/kg but from treatments in 0.5 mol/L NaOH and 4 mol/L NaOH respectively, the time required for measurement was far higher for the latter sample.

Thus, the conductometric titrations showed evidence of greater resistance to permeation of alkali through fibers carboxymethylated in baths with higher alkali content, and that it was not related solely to the degree of carboxymethylation. Carboxymethylation of cellulose significantly increases the swelling and gelation propensity (Thielking and Schmidt 2006). However, differences of permeation resistance were observed in cases where the degree of carboxymethylation was similar but the reaction conditions (i.e. alkali content in reaction media) were different, as highlighted in the discussion of conductometric titration results (*cf.* Fig. 9). The reason for this may originate from differences in topographical distribution of the substituted carboxymethyl groups within fiber structures as function of the reaction conditions. This aspect is being further explored through analysis of moisture sorption rates and equilibria from dynamic vapor sorption measurements, and through spatial mapping of carboxyl groups with FTIR microscopy and atomic force microscopy combined with FTIR spectroscopy.

Conclusions

The degree of carboxymethylation increased with NaOH content in reaction media. A higher temperature (50 °C vs. 30 °C) improved carboxymethylation yields when the NaOH concentration in media was at 0.5 mol/L, but when the NaOH concentration increased to 4 mol/L, the higher temperature yielded lower degree of carboxymethylation. When the reaction sequence consisted of first impregnating fibers with MCA and then adding alkali (the *rp* sequence) an improvement of carboxymethylation was observed in media containing 4 mol/L NaOH, but no effect of the reaction sequence was observed for reactions in 0.5 mol/L NaOH. Overall, the yield of carboxymethylation treatments in these experiments was low, with measured carboxymethyl contents accounting for about $0.2 - 1.6\%$ of the available MCA in reaction baths, or equivalent to average degrees of substitution in the range $0.01 - 0.11$. However, the results did yield interesting insights on performance of the carboxymethylated fibers, as measured by dye sorption.

The dye sorption levels were far below the total carboxyl content in all fibers, but there were differences between fibers carboxymethylated with different alkali contents. The fibers reacted in media containing 0.5 mol/L NaOH exhibited greater dye sorption levels compared to fibers reacted in 4 mol/L NaOH, despite the latter samples exhibiting greater carboxyl contents. There were indications of greater dye accumulation on the surfaces of fibers reacted in 4 mol/L NaOH. The observations point to greater resistance to dye permeation in fibers carboxymethylated in 4 mol/L NaOH. The observations from conductometric titrations supported the inference of differences in permeation resistance, but showed that it was not a function solely of the degree of carboxymethylation and that the content of NaOH during the derivatization role also had a role. The likely reason for this may stem from differences of topographical distribution of the substituted carboxymethyl groups as function of the reaction conditions. Supporting evidence for this hypothesis is being sought through tests of dynamic vapor sorption as well as through spatial mapping of carboxyl groups with atomic force microscopy combined with FTIR spectroscopy. Of interest will also be to understand the influence of alkali on extents of cellulose hydroxyl group accessibility to carboxymethylation, and further, of carboxymethyl group accessibility to adsorbates such as methylene blue.

Data availability Online Resource 1.pdf: Additional data from the results of fiber analyses. All data that support the findings of this study are available from the corresponding author, APM, upon reasonable request.

Declarations

Competing interests The authors declare no competing interests.

Ethical approval Not applicable, because this article does not contain any studies with human or animal subjects.

References

Anon (2023) Attenuated total reflection ATR: theory and applications, Madison, WI, USA. https://www.piketech.com/files/pdfs/PIKE_ATR_Theory-Applications.pdf. Accessed 30 Sep 2023

Bergeron JA, Singer M (1958) Metachromasy: an experimental and theoretical reevaluation. J Cell Biol 4:433–457. https://doi.org/10.1083/jcb.4.4.433

Carrillo F, Colom X, Suñol JJ, Saurina J (2004) Structural FTIR analysis and thermal characterisation of lyocell and viscose-type fibres. Eur Polym J 40:2229–2234. https://doi.org/10.1016/j.eurpolymj.2004.05.003

Chen J, Wu J, Raffa P et al (2022) Superabsorbent Polymers: from long-established, microplastics generating systems, to sustainable, biodegradable and future proof alternatives. Prog Polym Sci 125:101475. https://doi.org/10.1016/J.PROGPOLYMSCI.2021.101475

DIN (1985) 38405-1:1985-12: German standard methods for the examination of water, waste water and sludge; anions (group D); determination of chloride ions (D 1)

Fras L, Laine J, Stenius P et al (2004) Determination of dissociable groups in natural and regenerated cellulose fibers by different titration methods. J Appl Polym Sci 92:3186–3195. https://doi.org/10.1002/app.20294

Gago D, Chagas R, Ferreira LM et al (2020) A novel cellulose-based polymer for efficient removal of methylene blue. Membranes 10:13. https://doi.org/10.3390/membranes10010013

Global Market Insights (2021) Carboxymethyl cellulose market. https://www.gminsights.com/industry-analysis/carboxymethyl-cellulose-cmc-market. Accessed 6 June 2023

Gogna M, Goacher R (2018) Comparison of three Fourier transform infrared spectroscopy sampling techniques for distinction between lignocellulose samples. BioResources 13:846–860

Gu H, He J, Huang Y, Guo Z (2012) Water soluble carboxymethylcellulose fibers derived from alkalization-etherification of viscose fibers. Fibers Polym 13:748–753. https://doi.org/10.1007/S12221-012-0748-X/METRICS

Harrick NJ, du Pré FK (1966) Effective thickness of bulk materials and of thin films for internal reflection spectroscopy. Appl Opt 5:1739–1743. https://doi.org/10.1364/AO.5.001739

Heinze T, El Seoud OA, Koschella A (2018a) Cellulose activation and dissolution. In: Heinze T, El Seoud OA, Koschella A (eds) Cellulose derivatives: synthesis, structure, and properties. Springer International Publishing, Cham, pp 173–257

Heinze T, El Seoud OA, Koschella A (2018b) Etherification of cellulose. In: Heinze T, El Seoud OA, Koschella A (eds) Cellulose derivatives: synthesis, structure, and properties. Springer, Cham, pp 429–477

Ibrahim NA, Eid BM, Abd El-Ghany NA, Mabrouk EM (2020) Polyfunctional cotton cellulose fabric using proper biopolymers and active ingredients. J Text Inst 111:381–393. https://doi.org/10.1080/00405000.2019.1634459

IMARC (2022) Cellulose acetate market. https://www.imarcgroup.com/cellulose-acetate-market. Accessed 6 June 2023

Katz S, Beatson RP (1984) The determination of strong and weak acidic groups in sulfite pulps. Sven Papperstidning-Nordisk Cellul 87:48–53

Klemm D, Philipp B, Heinze T, et al (1998) Appendix to volume 1: experimental protocols for the analysis of cellulose. In: Comprehensive cellulose chemistry, pp 223–251

Krässig H, Schurz J, Steadman RG, et al (2004) Cellulose. In: Ullmann's encyclopedia of industrial chemistry. Wiley

Lawton JB, Phillips GO (1982) The rôle of water in the metachromatic reaction. Die Makromol Chemie 183:1497–1509. https://doi.org/10.1002/macp.1982.021830614

Li C, Ma H, Venkateswaran S, Hsiao BS (2020) Sustainable carboxylated cellulose filters for efficient removal and recovery of lanthanum. Environ Res 188:109685. https://doi.org/10.1016/j.envres.2020.109685

Li Z-W, Du Z-M, Wang Y-W et al (2022) Chemical modification, characterization, and activity changes of land plant polysaccharides: a review. Polymers 14:4161. https://doi.org/10.3390/polym14194161

Li Y, Zhang B, Li Y et al (2023) Carboxymethyl cellulose-polyethylene glycol/montmorillonite composite film and its absorption of methylene blue. Phys Status Solidi 220:2200788. https://doi.org/10.1002/pssa.202200788

Liao Y, Alam N, Fatehi P (2022) Semitransparent films from low-substituted carboxymethylated cellulose fibers. J Mater Sci 57:10407–10424. https://doi.org/10.1007/s10853-022-07262-0

Liu GL, Kazarian SG (2022) Recent advances and applications to cultural heritage using ATR-FTIR spectroscopy and ATR-FTIR spectroscopic imaging. Analyst 147:1777–1797. https://doi.org/10.1039/D2AN00005A

Liu Y, Wei Y, He Y et al (2023) Large-scale preparation of carboxylated cellulose nanocrystals and their application for stabilizing pickering emulsions. ACS Omega 8:15114–15123. https://doi.org/10.1021/acsomega.2c08239

Manian AP, Braun DE, Široká B, Bechtold T (2022) Distinguishing liquid ammonia from sodium hydroxide mercerization in cotton textiles. Cellulose 29:4183–4202. https://doi.org/10.1007/s10570-022-04532-7

Marchessault RH, Liang CY (1960) Infrared spectra of crystalline polysaccharides. III. Mercerized cellulose. J Polym Sci 43:71–84. https://doi.org/10.1002/pol.1960.1204314107

Mischnick P, Momcilovic D (2010) Chemical structure analysis of starch and cellulose derivatives. Adv Carbohydr Chem Biochem 64:117–210. https://doi.org/10.1016/S0065-2318(10)64004-8

Mohkami M, Talaeipour M (2011) Investigation of the chemical structure of carboxylated and carboxymethylated fibers from waste paper via XRD and FTIR analysis. BioResources 6:1988–2003

Nunn S, Nishikida K (2008) Advanced ATR correction algorithm. ThermoFisher application note AN50581_E 05/08M. Thermo Electron Scientific Instruments LLC, Madison, WI, USA

Pal MK (1958) Polyelectrolyte chromotropes in metachromacy: Part II. Die Makromol Chemie 28:91–95. https://doi.org/10.1002/macp.1958.020280109

Rácz I, Deák A, Borsa J (1995) Fibrous carboxymethylcellulose by pad roll technology. Text Res J 65:348–354. https://doi.org/10.1177/004051759506500607

Rafatullah M, Sulaiman O, Hashim R, Ahmad A (2010) Adsorption of methylene blue on low-cost adsorbents: a review. J Hazard Mater 177:70–80. https://doi.org/10.1016/J.JHAZMAT.2009.12.047

Siswanta D, Wahyuni R, Mudasir M (2020) Synthesis of glutaraldehyde-crosslinked carboxymethyl cellulose-polyvinyl alcohol film as an adsorbent for methylene blue. In: Key engineering materials. Trans Tech Publications Ltd., pp 35–42

Sjostrom E, Enstrom B (1966) A method for separate determination of sulpho and carboxyl groups in sulphite pulps. Sven Papperstidning-Nord Cellul 69:55

Stone AL (1967) Aggregation of cationic dyes on acid polysaccharides II. Quantitative parameters of metachromasy. Biochim Biophys Acta Gen Subj 148:193–206. https://doi.org/10.1016/0304-4165(67)90294-2

Stone AL, Bradley DF (1967) Aggregation of cationic dyes on acid polysaccharides I. Spectrophotometric titration with acridine orange and other metachromatic dyes. Biochim Biophys Acta Gen Subj 148:172–192. https://doi.org/10.1016/0304-4165(67)90293-0

TAPPI (2008) T 237 cm-08: carboxyl content of pulp

Thakur D, Seo S, Hyun J (2023) Three-dimensional triboelectric nanogenerator with carboxymethylated cellulose nanofiber and perfluoroalkoxy films. J Ind Eng Chem 123:220–229. https://doi.org/10.1016/j.jiec.2023.03.037

Thielking H, Schmidt M (2006) Cellulose ethers. In: Ullmann's encyclopedia of industrial chemistry. Wiley

Wang J, Liu M, Duan C et al (2019) Preparation and characterization of cellulose-based adsorbent and its application in heavy metal ions removal. Carbohydr Polym 206:837–843. https://doi.org/10.1016/j.carbpol.2018.11.059

Wang Z, Jiang Y, Mao L et al (2023) Pilot-scale preparation of cellulose/carboxymethylcellulose composite fiber for methylene blue adsorption. Cellulose 30:3611–3623. https://doi.org/10.1007/s10570-023-05109-8

Wang Y (2017) How to choose proper FTIR spectroscopic techniques to analyze petroleum products. https://www.agilent.com/cs/library/eseminars/public/Molecular_Spectroscopy_FTIR_Oil_Analysi.pdf. Accessed 5 Dec 2023

Yan H, Zhang W, Kan X et al (2011) Sorption of methylene blue by carboxymethyl cellulose and reuse process in a secondary sorption. Coll Surf A Physicochem Eng Asp 380:143–151. https://doi.org/10.1016/j.colsurfa.2011.02.045